ELSEVIER

Chemical Engineering Journal 81 (2001) 23–34

Chemical Engineering Journal

www.elsevier.com/locate/cej

Pressure drop in fixed-bed adsorbers

M.H. Chahbani [a,*,1], D. Tondeur [b]

[a] *Institut National de Recherche Scientifique et Technique, BP 95 2050 Hammam-Lif, Tunisia*

[b] *Laboratoire des Sciences du Génie Chimique, CNRS-ENSIC, 1 Rue Grandville-BP, 451-54001 Nancy Cedex, France*

Received 30 September 1999; received in revised form 17 March 2000; accepted 10 May 2000

Abstract

The effect of pressure drop on the dynamic behavior of a fixed-bed adsorber during adsorption and desorption steps is studied for two operating modes (constant volume and molar flow rate at the bed inlet). For saturation with a constant volume flow rate, neglecting pressure drop gives rise to a late breakthrough for the concentration wave compared to the case with ΔP, in other words, overestimates the breakthrough time. This is essentially due to the increase in molar flow at the bed entrance inherent to the appearance of an axial pressure gradient. On the other hand, when a molar flow rate is maintained constant at the bed inlet, it is shown that neglecting pressure drop leads to an underestimation of the breakthrough time.

For the desorption step using a constant volume flow rate, it is seen that pressure drop engenders a shortening of regeneration. This apparent result is misleading. In fact, when reasoning in terms of gas quantity needed to regenerate the bed, it appears that pressure drop leads to an overconsumption of desorbing gas. This is confirmed when working with a constant molar flow rate. Thus, as intuitively expected, pressure drop is unfavorable to regeneration.

Keywords: Pressure drop; Fixed-bed absorber; Adsorption; Desorption

1. Introduction

Nowadays, pressure swing adsorption (PSA) is widely recognized as a viable solution to gas separation. Despite the large use of this separation technique, the theoretical understanding of the different phenomena involved is to be improved in order that the choice of operating conditions would be optimal. As a result, one can avoid resorting to empirical laws to scale up PSA industrial plants.

The present paper addresses the issue of the effect of pressure drop on adsorption and desorption. In many previous works, it has been supposed that the bed pressure drop is negligible. This hypothesis is surely not valid for processes such as rapid pressure swing adsorption (RPSA), which combine high flow rates and very small particle diameters.

The use of small adsorbent particles aims to reduce mass transfer resistances. To improve the productivity, the duration of the whole process is considerably reduced. This imposes, of course, very high velocities. However, the effect of pressure drop along the bed is more important when the cycle time decreases.

The first studies dealing with pressure drop were carried out by Zwiebel [1] and Zwiebel and Schnitzer [2]. These works are limited to dilute mixtures. In this case, one can neglect the effect of adsorption on velocity, thus permitting to get analytical expressions for both pressure and velocity. The more interesting result of these studies is that pressure drop causes an earlier breakthrough of the concentration wavefront compared to the case with no ΔP.

Doong and Yang [3] studied the role of pressure drop in PSA. They concluded that, in conventional multibed PSA, the net effect of pressure drop is increasing the light product purity and decreasing recovery for the same throughput.

Buzanowski et al. [4] confirmed that pressure drop does only contribute to the broadening of the breakthrough curve. Their experimental results for both adsorption and desorption agree well with simulations.

Kikkinides and Yang [5] studied the effect of pressure drop on the dynamics of isothermal and adiabatic adsorbers. Their simulation and experimental results are in accordance with those of Zwiebel [1] and Zwiebel and Schnitzer [2], that is, an earlier breakthrough in the presence of pressure drop.

Lu et al. [6] studied the impact of intraparticle convection on the desorption of gases from fixed beds with ‘large-pore’ adsorbents.

* Corresponding author. Present address: Department de genie chimique-GRESIP, Ecole Polytechnique Montreal, C.P. 7079, succ.centre-ville, Montreal, Que., Canada H3C 3A7. Tel.: +1-514-3405794; fax: +1-514-3404063.

E-mail address: chahbani@visto.com (M.H. Chahbani).

[1] Tel.: +90-216-1-430053/430044; fax: +90-216-1-430934 (Institut National de Recherche Scientifique et Technique, Tunisia).

1385-8947/01/$ – see front matter
PII: S1385-8947(00)00215-1

Nomenclature

b	parameter of Langmuir isotherm (Pa^{-1})
C	bulk phase concentration (mol/m^3)
cp	heat capacity (J/mol K or J/kg K)
D_{ax}	mass axial dispersion coefficient (m^2/s)
D_{col}	column diameter (m)
d_p	particle diameter (m)
L	bed length (m)
N_c	number of cells
N_g	number of species in the gas mixture
P	total pressure (Pa)
Q_m	parameter of Langmuir isotherm (mol/kg)
q	adsorbed phase concentration (mol/m^3)
R	gas constant (J/mol K)
u	interstitial velocity (m/s)
T	temperature (K)
t	time (s)
Z	compressibility factor of the gas mixture
z	axial coordinate in the bed (m)

Greek letters

ϵ	interparticle porosity
ϵ_p	intraparticle porosity
ϵ_t	total porosity
μ	fluid viscosity (kg/m s)
ρ	fluid density (kg/m^3)

Superscripts

$*$	equilibrium
i	refers to species i

Subscripts

a	refers to adsorbed phase
feed	at the bed entrance
g	refers to gas phase
i	refers to species i
out	at the bed exit
p	refers to adsorbent particle
s	refers to solid phase
0	initial condition

It is to be noted that large effects of pressure drop on pressurization and blowdown steps in PSA cycles were found and discussed [7–15].

The present paper aims at giving further clarifications concerning the dynamic bed behavior during adsorption and desorption steps when pressure drop is significant, under conditions of high adsorptive concentration, and therefore, of important velocity changes due to adsorption.

2. Modeling

The numerical simulation of an adsorption or desorption step, assuming no mass transfer resistances between gas and solid phases, involves the solution of mass, heat and momentum balances.

2.1. Mass balance in packed bed

The differential fluid phase mass balance for the component i is given by the following axially dispersed plug flow equation:

$$\epsilon_t \frac{\partial C y_i}{\partial t} + (1-\epsilon)\frac{\partial q_i^*}{\partial t} + \frac{\partial(\epsilon u C y_i)}{\partial z} = \frac{\partial}{\partial z}\left(\epsilon D_{ax} C \frac{\partial y_i}{\partial z}\right) \quad (1)$$

The overall mass balance for the bulk gas is given by

$$\epsilon_t \frac{\partial C}{\partial t} + (1-\epsilon)\sum_{i=1}^{N_g}\frac{\partial q_i^*}{\partial t} + \frac{\partial(\epsilon u C)}{\partial z} = 0 \quad (2)$$

where u is the interstitial fluid velocity, ϵ the bed or the interparticle void fraction and $C = ZP/RT$, with Z being the compressibility factor of the gas mixture.

2.2. Heat balance

In general, adsorbers are far from being isothermal due to heat of adsorption. A heat balance for the bed can be written as

$$\epsilon_t \frac{\partial(CH_g)}{\partial t} + (1-\epsilon)\frac{\partial(uCH_g)}{\partial z} + (1-\epsilon)\left(\rho_s \frac{\partial H_s}{\partial t} + \sum_{i=1}^{N_g} q_i^* \frac{\partial H_a^i}{\partial t}\right) - (1-\epsilon)\sum_{i=1}^{N_g}\Delta H_i \frac{\partial q_i^*}{\partial t} + \frac{4h}{D_{col}}(T - T_e) = 0 \quad (3)$$

with

$$dH_g = \sum_{i=1}^{N_g} cp_g^i \, dT, \qquad dH_a^i = cp_a^i \, dT, \qquad dH_s = cp_s \, dT \quad (4)$$

In the following, the heat capacities of adsorbed species (cp_a^i) are supposed to be equal to those in gas phase (cp_g^i).

2.3. Momentum balance

Ergun's law is used to estimate locally the bed pressure drop:

$$-\frac{\partial P}{\partial z} = 150.0\frac{(1-\epsilon)^2}{\epsilon^2}\frac{\mu}{d_p^2}u + 1.75\frac{1-\epsilon}{\epsilon}\frac{\rho}{d_p}u^2 \quad (5)$$

where μ is the gas mixture viscosity, ρ the gas density and where d_p is the particle diameter.

In addition to Ergun's law, another model considering that the pressure is uniform in the bed (negligible pressure drop), will be used.

In the latter model, the velocity is not constant, but varies with axial distance due to adsorption.

3. Boundary conditions

It is important to define precisely the operating mode followed during the adsorption operation in order that simulations represent fairly well the experiments. In fact, the operating mode fixes the boundary conditions to be considered in the modeling. Two operating modes are going to be used herein. The differences between the two modes concern the nature of flow rate imposed at the bed inlet (volume and molar flow rate). In practice, this corresponds to the use of volume or mass flowmeters. Of course, if the pressure drop is supposed negligible along the bed, there is no need to distinguish the two cases; the use of either flow rate then leads to the same results.

- Constant volume flow rate:

$$z = 0 \quad u = u_{\text{feed}},\ y_i = y_{i_{\text{feed}}},\ T = T_{\text{feed}} \quad \forall t$$
$$z = L \quad P = P_{\text{out}} \quad \forall t$$

- Constant molar flow rate:

$$z = 0 \quad uC = F_{\text{feed}},\ y_i = y_{i_{\text{feed}}},\ T = T_{\text{feed}} \quad \forall t$$
$$z = L \quad P = P_{\text{out}} \quad \forall t$$

In the two cases, the pressure at the bed outlet as well as the composition and temperature of the gas mixture at the bed inlet are maintained constant.

4. Numerical method

The foregoing models require the simultaneous solution of a set of partial differential and algebraic equations (overall and component mass balance equations, heat balance equation and momentum balance equation). The above equations are written in dimensionless form. The well-mixed cells method is used to discretize the system. It consists of dividing the domain in a series of N_c perfectly stirred cells, each cell being of length Δz. The resulting system of ordinary differential and algebraic equations are solved by the DASSL integration algorithm of Petzold [16] which is based on a modified version of Newton's method. Axial dispersion within the packed bed is assessed by the choice of a suitable number of cells, thus eliminating the need for the axial dispersion terms appearing in the governing equations. For all the following simulations, the Peclet number $P_e = uL/D_{ax}$ is equal to 100, which corresponds to $N_c = 50$ cells ($P_e = 2N_c$).

5. Results and discussion

The numerical simulations presented herein deal with the separation of a two-component mixture (H_2 and CH_4) by using activated carbon. H_2 is supposed to be a non-adsorbed species. The adsorption equilibrium isotherm of CH_4 on activated carbon is given by the Langmuir model

$$Q^* = \frac{Q_m b y_i P}{1 + b y_i P} \tag{6}$$

The parameters Q_m and b are functions of temperature:

$$Q_m = k_1 - k_2 T \tag{7}$$

$$b = k_3 \exp\left(\frac{k_4}{T}\right) \tag{8}$$

Table 1 gives the values of k_i parameters and adsorption heat used in simulations [17]. These values are obtained by fitting experimental isotherms. Other physical properties of activated carbon are given in Table 2 [17].

The model requires the assessment of the physical properties of the gas mixture. The compressibility factor is calculated following the method of Lee-Keesler [18]. The viscosity of each pure gas is estimated by the Lucas method [18], whereas the viscosity of the mixture is evaluated by the Reichenberg method [18]. The compressibility factor (Z), the mixture viscosity (μ) as well as the gas density (ρ) vary with temperature, pressure and composition; therefore, they are calculated at every computation step.

The heat capacities of the various gases are calculated by using an equation of the following form:

$$\text{cp(J/mol K)} = a + bT + cT^2 + dT^3 \tag{9}$$

The constants a, b, c and d for the two gases are listed in Table 3.

Table 1
Langmuir parameters and adsorption heat

Langmuir parameters	
k_1	7.063×10^3 mol/m^3
k_2	13.610 mol/m^3 K
k_3	3.071×10^{-8} Pa^{-1}
k_4	1574.1 K
Adsorption heat (ΔH)	20.0 kJ/mol

Table 2
Adsorbent physical properties

Apparent density (ρ_p)	830 kg/m^3
Intraparticle porosity (ϵ_p)	0.6
Particle diameter (d_p)	0.2×10^{-3} m
Heat capacity (cp_s)	1.050 kJ/kg K

Table 3
a, b, c and d constants for the calculation of heat capacities

	a	b	c	d
H_2	27.14	9.274×10^{-3}	-1.381×10^{-5}	7.645×10^{-8}
CH_4	19.25	5.213×10^{-2}	1.197×10^{-5}	-1.132×10^{-8}

Table 4
Operating conditions used in the simulations

Initial pressure (P_0)	
Adsorption step	20.0×10^5 Pa
Desorption step	1.0×10^5 Pa
Initial temperature	298 K
Feed temperature	298 K
CH_4 mole fraction in feed	
Adsorption step	0.3
Desorption step	0.0
Column length (L)	5.0 m
Interparticle porosity (ϵ)	0.4
Superficial velocity (ϵu)	0.3 m/s

Table 4 gives the operating conditions used for computations.

According to Ergun's correlation, the parameters that affect pressure drop are particle diameter, flow velocity, interparticle porosity and column length. In order to create a significant pressure drop along the bed, a small particle diameter and a high gas velocity are used. Such conditions are commonly utilized in RPSA. Unless otherwise stated, the following simulations are in the adiabatic case ($h = 0$).

6. Adsorption step

The bed is initially devoid of any traces of methane. It contains pure hydrogen at 20 bar and 298 K.

Fig. 1 shows breakthrough curves of methane obtained in the cases where the pressure drop is either taken into account or neglected. In a first approach, constant volume flow rate at the bed inlet is assumed. It can be seen that the presence of a pressure gradient along the bed gives rise to an earlier breakthrough. This result agrees with those of Zwiebel [1], Zwiebel and Schnitzer [2], Doong and Yang [3] and Kikkinides and Yang [5]. According to Doong and Yang [3], pressure drop reduces the bed adsorption capacity. As a result, the breakthrough time decreases. This explanation is wrong as will be seen later. Kikkinides and Yang explained the earlier breakthrough by the fact that the concentration wavefront velocity increases along the bed due to gas expansion which is the consequence of pressure drop. This is in part true as can be noticed in Fig. 2 which gives the evolution of the axial gas velocity during the adsorption step. The reduced velocity is defined as the ratio of the local velocity to the inlet velocity (u_{feed}). The latter figure is obtained for isothermal conditions in order to see the sole effect of pressure drop on velocity. The velocity undergoes a sharp decrease in the mass transfer zone. Before and after this zone, it increases gradually as gas passes through regions of lower pressure. The lowest pressure is of course at the bed outlet. This observation is better seen in Fig. 3 which gives the gas velocity at the bed outlet obtained with and without pressure drop. For the model with no pressure drop, velocity is only affected by adsorption; thus before and after the mass transfer zone, velocity is constant.

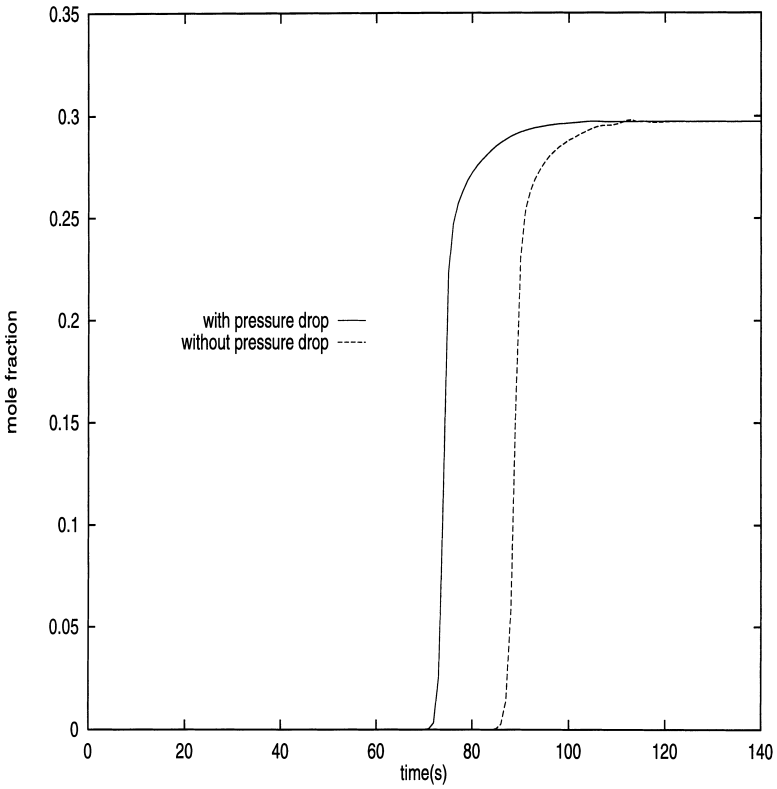

Fig. 1. Comparison of the breakthrough curves with and without pressure drop for constant volume flow rate at the bed inlet.

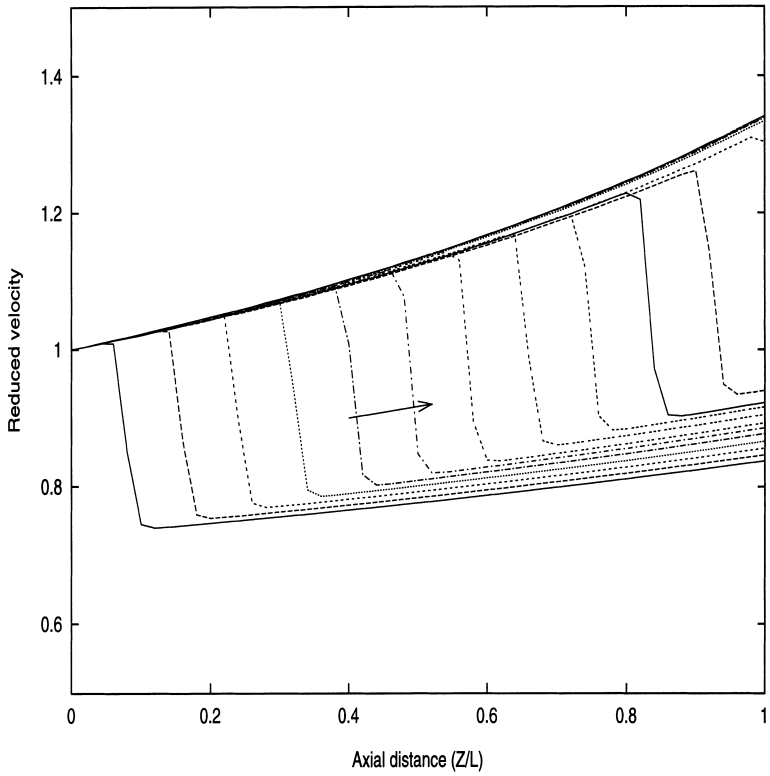

Fig. 2. Axial profiles of reduced velocity for different times ($\Delta t = 7.5\,\mathrm{s}$) during adsorption, constant volume flow rate at the bed inlet. Arrow indicates increasing time.

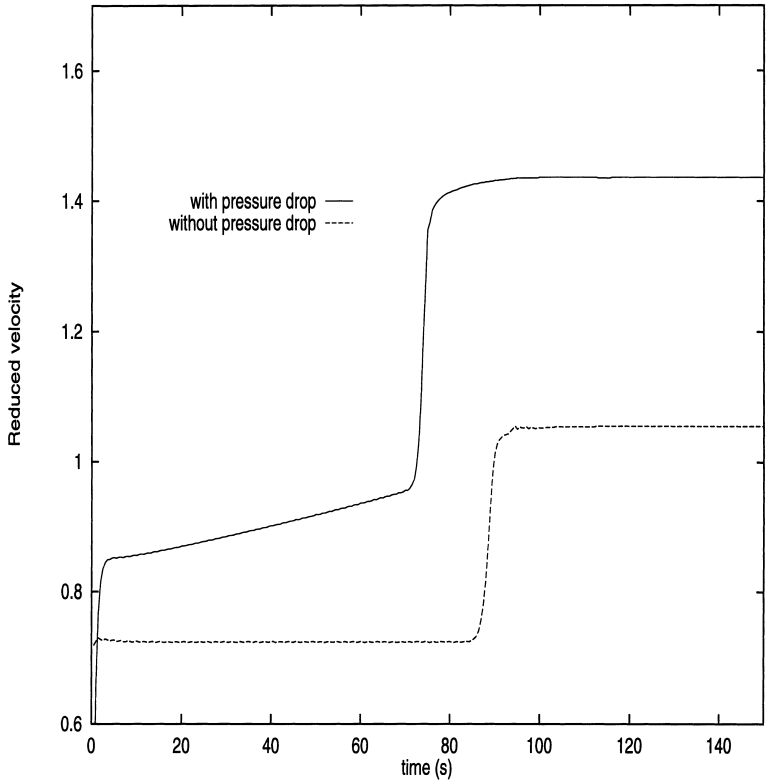

Fig. 3. Reduced velocity at the bed exit with and without pressure drop during adsorption for constant volume flow rate at the bed inlet.

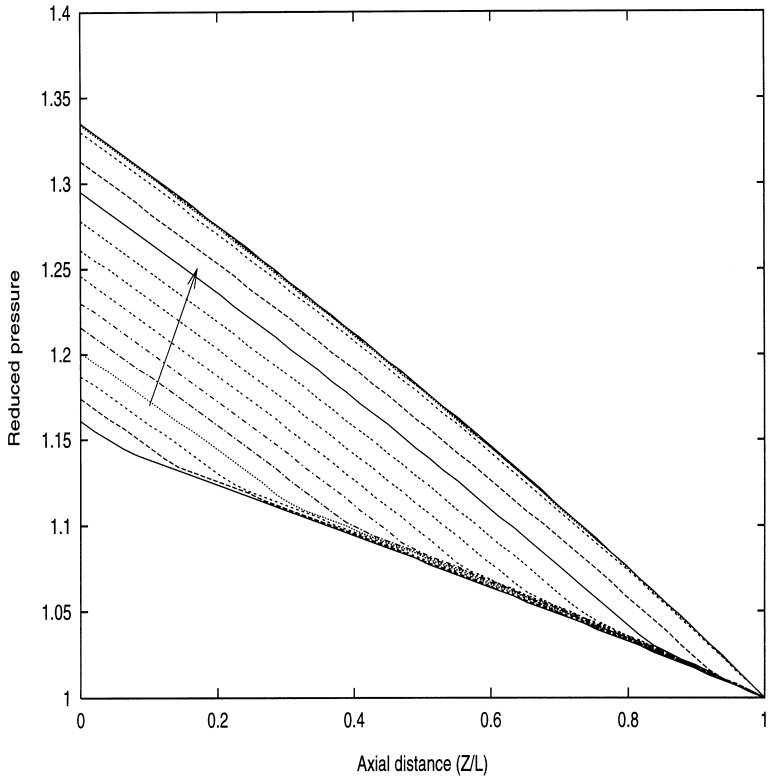

Fig. 4. Axial profiles of reduced pressure for different times ($\Delta t = 7.5$ s) during adsorption, constant volume flow rate at the bed inlet. The arrow indicates the direction of increasing times.

As the concentration wave moves towards the bed exit, the pressure increases continuously (Fig. 4). Reduced pressure is defined as local pressure divided by pressure at the bed exit (maintained constant = initial pressure). A final profile is reached when the column is completely saturated. Before the bed is totally saturated, the axial pressure profile is made up of two linear parts. The change of slope is located in the mass transfer zone where a significant decrease in gas velocity occurs due to adsorption. For dilute mixtures, the gas velocity is much less affected by adsorption and the axial pressure profile would be composed of two linear curves with nearly identical slopes.

Another important factor that contributes to the earlier breakthrough is the increase in molar flow at the column inlet. In fact, it is worth noting that, due to the variation of pressure at the bed entrance, although volume flow is constant, the molar flow is not constant but increases with time. Therefore, it is more appropriate from a practical point of view to compare breakthrough curves taking as x-coordinate the quantity of adsorbable gas introduced in the column, instead of time, as shown in Fig. 5. It appears clearly that, despite the earlier breakthrough on a time scale, in the presence of pressure drop, the amount of adsorbable gas loaded is greater. The difference between the two curves represents the increase in the bed adsorption capacity resulting from the overall increase in the bed pressure.

Neglecting pressure drop when it is significant results in an overestimation of the breakthrough time. In practice, this would inevitably lead to a loss in purity as a non-negligible quantity of the heavy component is allowed to leave the bed during the production step, thus contaminating the collected pure product.

Pressure drop also implies a higher energy cost and more severe mechanical problems in the design of the adsorbent and adsorber. Aside from these negative aspects, the inlet pressure increase necessitated by pressure drop could have a beneficial effect on the productivity of the PSA cycle insofar as it reduces the production step duration. Nevertheless, this should be considered with precaution because, at the same time, pressure drop does increase notably the duration of pressurization and blowdown steps as well. The impact of pressure drop on the regeneration step will be addressed in the following part of this paper. It follows that the whole PSA cycle should be studied in detail so as to see the global effect of pressure drop on the process productivity.

It is interesting to note that feed composition has an enormous influence on the final pressure profile along the bed (Fig. 6). The final profile is obtained when the bed is saturated (there are no longer any velocity variations due to adsorption).

The differences obtained stem solely from the variability of feed physical properties, namely density and viscosity. These properties have a direct impact on the momentum balance equation (Ergun's correlation). In the case under study, the two components of feed (hydrogen and methane) have significantly different physical properties. The higher

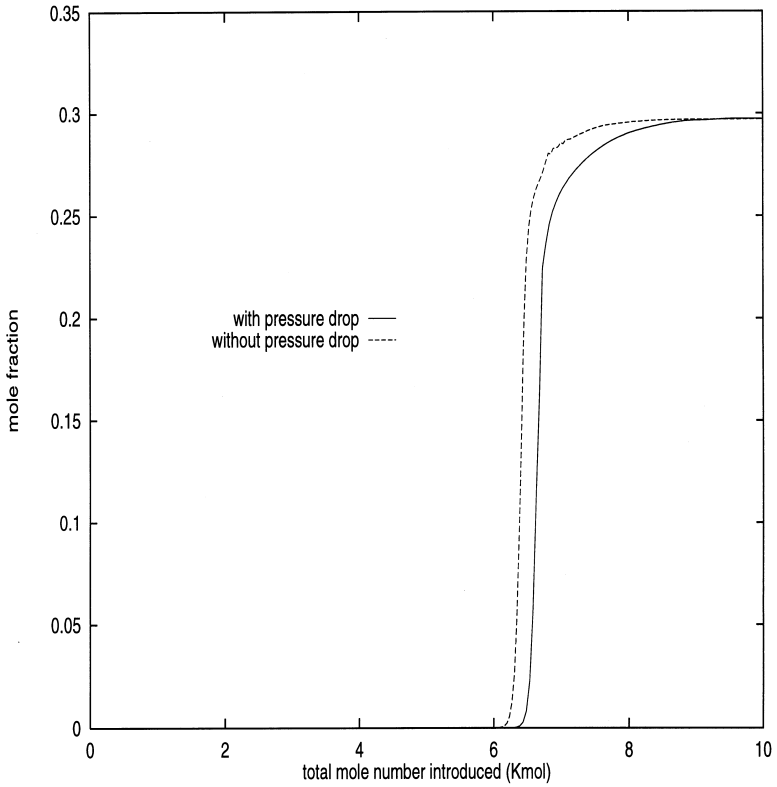

Fig. 5. Histories of adsorbable species mole fraction, at the bed exit with and without pressure drop during adsorption, as a function of the total mole number introduced in the bed, constant volume flow rate at the bed inlet.

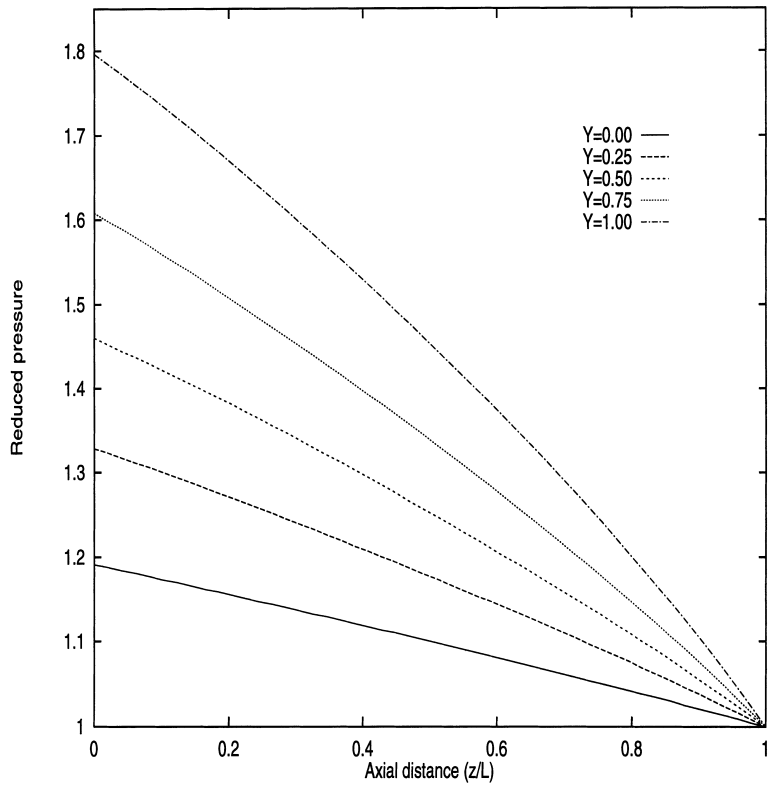

Fig. 6. Final axial pressure profile for different feed compositions during adsorption, constant volume flow rate at the bed inlet.

the mole fraction of the adsorbable gas (methane) in the feed, the larger the pressure drop across the column. Pressure drop represents 19% of the initial pressure (pressure at the bed outlet) for a pure hydrogen feed and 79.6% for a pure methane one. However, this evolution trend could be in the opposite direction. In fact, this depends solely upon the physical properties of constituents composing the gas mixture. If these properties are maintained constant during the whole process, this could lead to errors in simulation results, especially for steps which are accompanied by notable variations of gas composition, temperature and pressure (blowdown, regeneration). The physical properties vary with the aforementioned parameters; this is why they should be evaluated at each computational step.

It is worthwhile to note that if Darcy's law was used instead of Ergun's law as momentum balance (only viscosity is taken into account, neglecting density), pressure drop would have represented 15 and 20% of the initial pressure for feeds of pure hydrogen ($\mu = 0.91 \times 10^{-3}$ kg/m s at 298 K and 20 bar) and methane ($\mu = 1.13 \times 10^{-3}$ kg/m s at 298 K and 20 bar), respectively. Comparing pressure drop values obtained with the two momentum equations (Darcy and Ergun) for a pure methane feed demonstrates that the inertial term in Ergun's correlation (second term) could play a significant role in increasing bed resistance to flow.

Let us consider now the case where the molar flow rate is maintained constant at the bed inlet. The value of this flow rate is equal to the one obtained when pressure drop is neglected (in this case, pressure and velocity at the bed entrance remain constant during the whole step) in order that the comparison would be meaningful. As was said previously, if there is no pressure drop along the column, imposing either volume or molar flow rate gives the same simulation results. So one can resort to either boundary condition (volume or molar flow rate at column inlet) to simulate an adsorption step in the absence of pressure drop.

The axial profiles of reduced velocity at different times during adsorption (in the isothermal case) are given in Fig. 7. The evolution of pressure is similar to the one shown in Fig. 4 obtained for a constant volume flow rate. Note that the gradual increase in pressure at the bed inlet is accompanied by a gradual decrease in velocity, thus permitting to maintain the molar flow rate constant during the entire step.

Breakthrough curves of methane, with and without pressure drop, are given in Fig. 8 . The breakthrough time in the case with pressure drop is larger than with a uniform axial pressure. As a matter of fact, the increase in bed adsorption capacity (due to the appearance of a pressure gradient across the column and the increase in the mean pressure) on one hand, and the decrease in gas velocity on the other hand, are both acting in the same direction, that is, the slowing of the concentration wavefront.

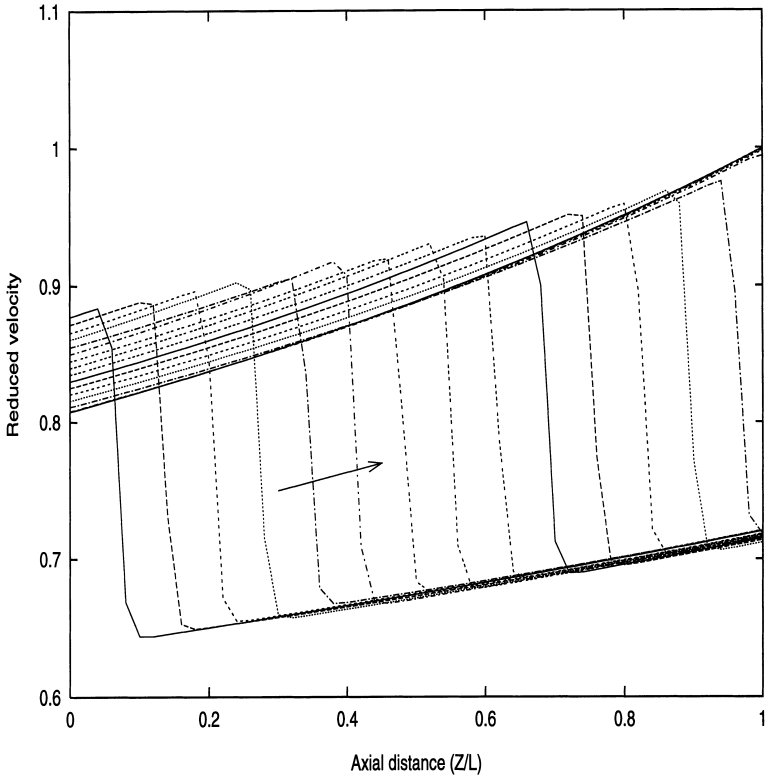

Fig. 7. Axial profiles of reduced velocity for different times ($\Delta t = 7.5$ s) during adsorption, constant molar flow rate at the bed inlet.

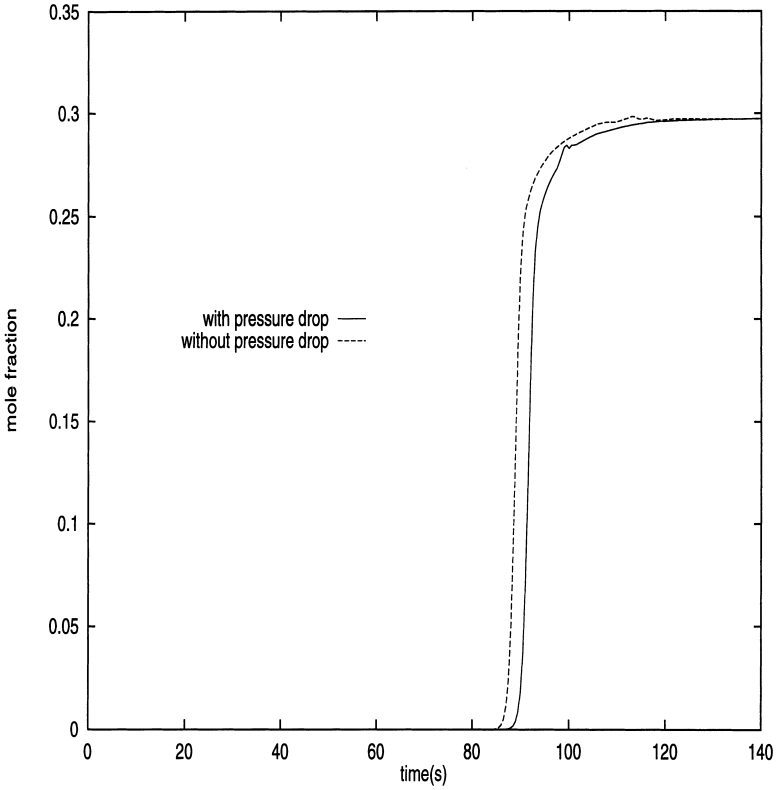

Fig. 8. Comparison of the breakthrough curves with and without pressure drop during adsorption for constant molar flow rate at the bed inlet.

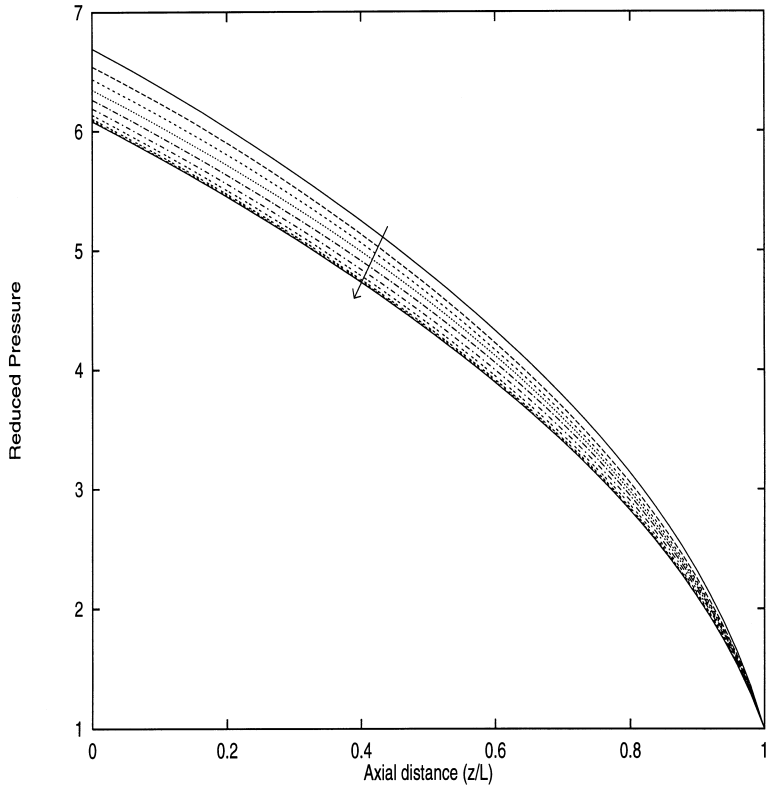

Fig. 9. Axial profiles of reduced pressure for different times ($\Delta t = 40$ s) during desorption, constant volume flow rate at the bed inlet. Arrow indicates increasing time.

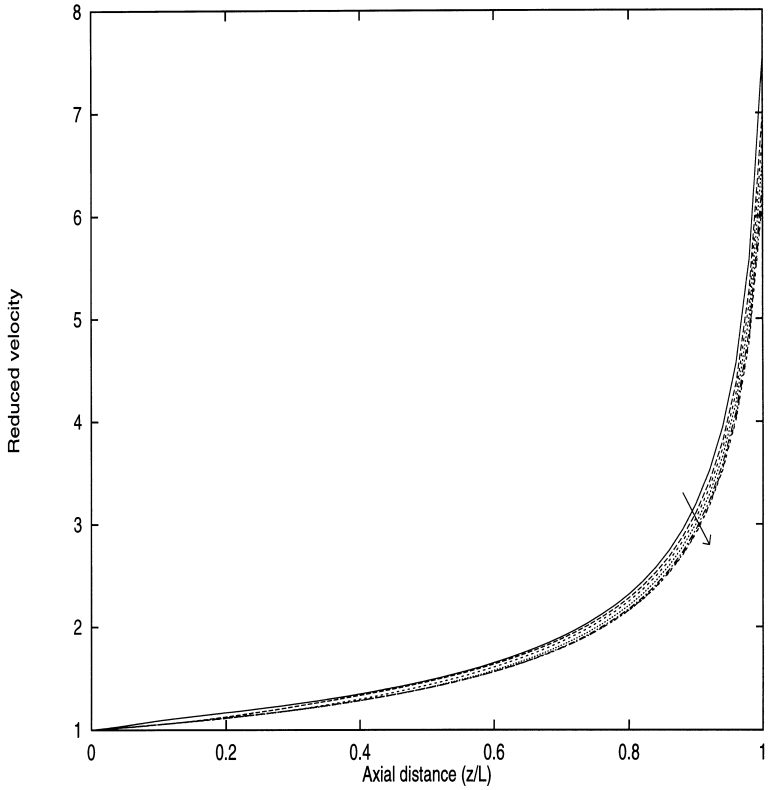

Fig. 10. Axial profiles of reduced velocity for different times ($\Delta t = 80$ s) during desorption, constant volume flow rate at the bed inlet. Arrow indicates increasing time.

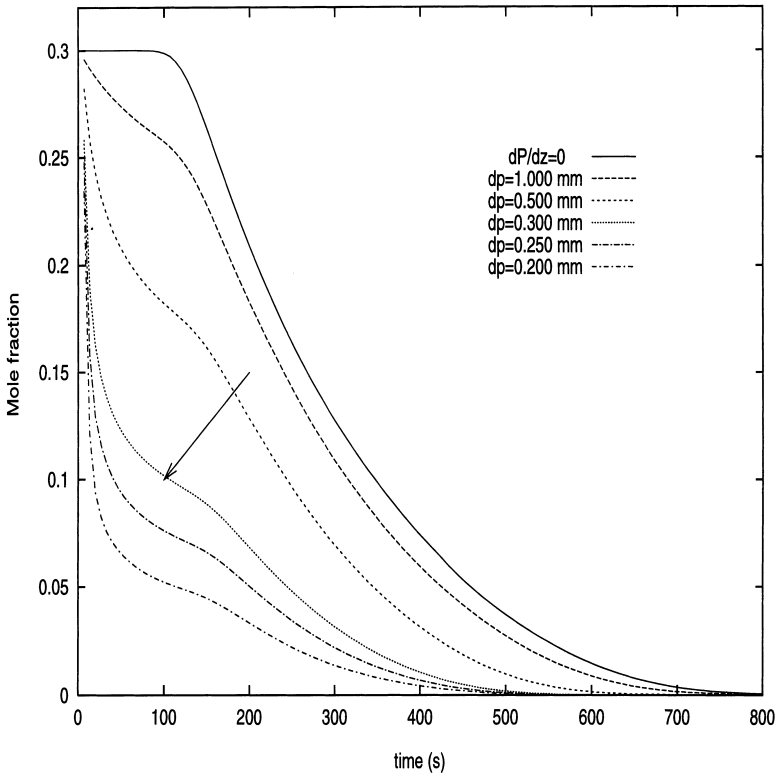

Fig. 11. Histories of adsorbable species mole fraction during desorption at the bed exit for different values of pressure drop, constant volume flow rate at the bed inlet. Arrow indicates direction of decreasing particle size.

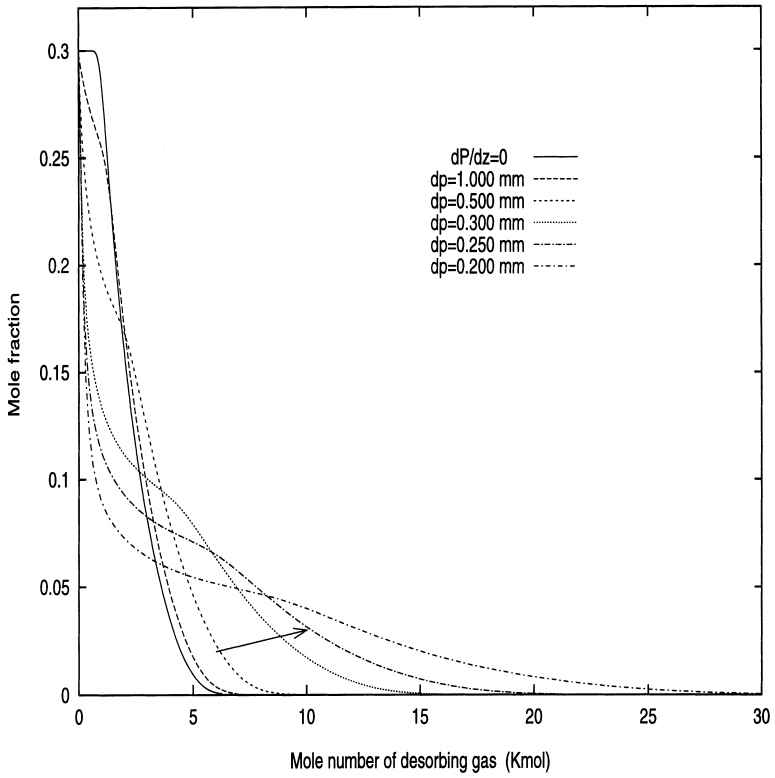

Fig. 12. Histories of adsorbable species mole fraction during desorption at the bed exit for different particle sizes during desorption as a function of desorbing gas mole number, constant volume flow rate at the bed inlet. Arrow indicates decreasing particle size.

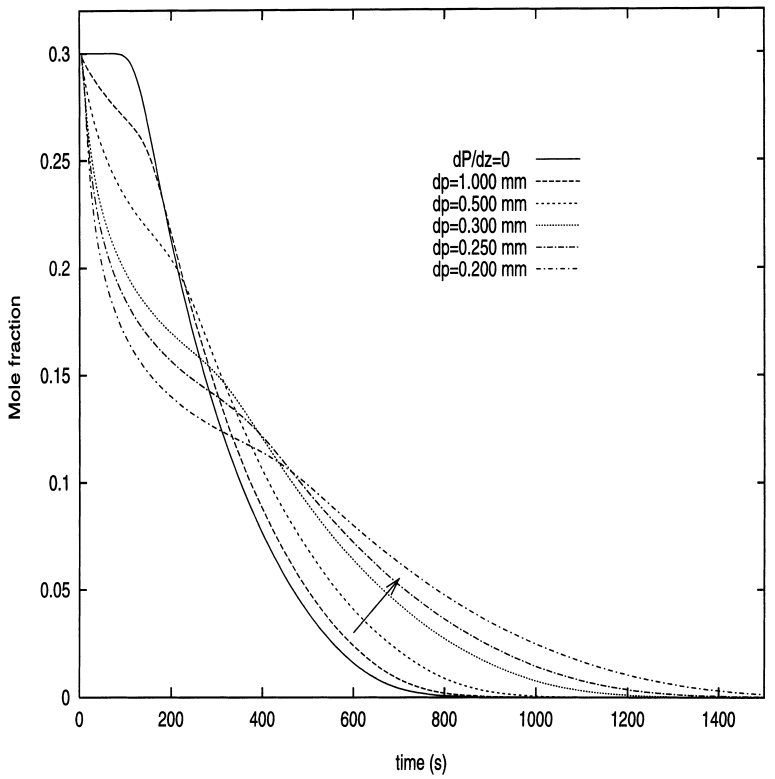

Fig. 13. Histories of adsorbable species' mole fraction at the bed exit for different particle sizes during desorption, constant molar flow rate at the bed inlet. Arrow indicates decreasing particle size.

7. Desorption step

Initially, the bed is uniformly loaded ($P = 1$ bar, $y_{CH_4} = 0.3$, $T = 298$ K). This means that the bed was saturated with a very slow flow to ensure a negligible pressure gradient along the bed.

The change with time of axial pressure and velocity is given in Figs. 9 and 10, respectively, for the case of a constant volume flow rate (for isothermal conditions). As regeneration progresses, pressure drop decreases owing to the variation of gas physical properties which are related to the mixture composition. Pressure and velocity attain final states when the bed is totally purged.

Fig. 11 represents desorption curves for the isobaric case (no pressure drop) as well as for several particle diameters (different values of pressure drop). The study of the above-mentioned figure shows that the greater the pressure drop (i.e. the smaller the particle diameter), the shorter the regeneration of the bed. Based on this finding, one can conclude that pressure drop is a desirable phenomenon for it facilitates desorption by allowing to get a substantial decrease in the regeneration duration, that is, a better productivity. For this reason, Doong and Yang [3] consider that pressure is helpful to desorption. However, one should not be deceived by this apparent advantage. In fact, as done for the adsorption step, let us compare the desorption curves after substituting the quantity of pure hydrogen (used to regenerate the bed) for time in the x-axis as shown in Fig. 12. This substitution is carried out so as to take into account the variation of molar flow rate at the bed inlet. It can be noticed that the consumption of pure hydrogen increases enormously with pressure drop. So the appearance of an axial pressure gradient due to bed resistance to flow is unfavorable for desorption. It engenders not only a higher energy cost but also a higher amount of regenerating gas.

The preceding findings are better illustrated when using a constant molar flow rate. In fact, from Fig. 13 which gives several desorption curves in the presence and absence of pressure drop, it is visible that as pressure drop increases, the regeneration step becomes longer with a more elongated tail.

8. Conclusion

The impact of pressure drop on the dynamic behavior of a fixed-bed adsorber during adsorption and desorption steps was studied. Two operating modes were considered: constant volume and molar flow rate at the bed inlet. Concerning saturation with a constant volume flow rate, taking into account pressure drop results in an early breakthrough for the concentration wave compared to the case with a uniform axial pressure. This is due to the increase in molar flow inherent to the appearance of an axial pressure gradient. When a molar flow rate is maintained constant at the bed entrance, it was shown that neglecting pressure drop leads to an underestimation of the breakthrough time.

For regeneration, the use of a constant volume flow rate engenders a shortening of the step duration. This apparent result is misleading. In fact, when reasoning in terms of gas quantity needed to regenerate the bed, it appears that pressure drop leads to an overconsumption of desorbing gas. This is confirmed when working with a constant molar flow rate. Thus, pressure drop has a negative effect on regeneration.

References

[1] I. Zwiebel, Fixed bed adsorption with variable gas velocity due to pressure drop, Ind. Eng. Chem. Fundam. 8 (1969) 803–807.
[2] I. Zwiebel, J.J. Schnitzer, AIChE Symp. Ser. 69 (134) (1973) 18–24.
[3] S.J. Doong, R.T. Yang, The role of pressure drop in Pressure Swing Adsorption, AIChE Symp. Ser. 84 (1988) 145–154.
[4] M.A. Buzanowski, R.T. Yang, O.W. Haas, Direct observation of the effects of bed pressure drop on adsorption and desorption, Chem. Eng. Sci. 44 (10) (1989) 2392–2394.
[5] E.S. Kikkinides, R.T. Yang, Effects of bed pressure drop on isothermal and adiabatic adsorber dynamics, Chem. Eng. Sci. 48 (9) (1993) 1545–1555.
[6] Z. Lu, J.M. Loureiro, M.D. LeVan, A.E. Rodrigues, Effect of intraparticle forced convection on gas desorption from fixed beds containing 'Large-pore' adsorbents, Ind. Eng. Chem. Res. 31 (1992) 1530–1540.
[7] J. Hart, M.J. Battrum, W.J. Thomas, Axial pressure gradients during the pressurization and depressurization steps of a PSA gas separation cycle, Gas Sep. Purif. 4 (1990) 97–102.
[8] Z.P. Lu, J.M. Loureiro, A.E. Rodrigues, Pressurization and blowdown of adsorption beds. II. Effect of the momentum and equilibrium relations on isothermal operation, Chem. Eng. Sci. 48 (9) (1993) 1699–1707.
[9] Z.P. Lu, J.M. Loureiro, M.D. LeVan, A.E. Rodrigues, Dynamics of pressurization and blowdown of an adiabatic bed. III, Gas Sep. Purif. 6 (1) (1992) 15–23.
[10] Z.P. Lu, J.M. Loureiro, M.D. LeVan, A.E. Rodrigues, Dynamics of pressurization and blowdown of an adiabatic adsorption bed. 4. Intraparticle diffusion/convection models, Gas Sep. Purif. 6 (2) (1992) 89–100.
[11] Z.P. Lu, J.M. Loureiro, M.D. LeVan, A.E. Rodrigues, Intraparticle convection effect on pressurization and blowdown of adsorbers, AIChE J. 38 (6) (1992) 857–867.
[12] A.E. Rodrigues, Z.P. Lu, J.M. Loureiro, M.D. LeVan, Simulated pressurization of adsorption beds, Gas Sep. Purif. 5 (1991) 115–124.
[13] C. Sereno, A.E. Rodrigues, Can steady-state momentum equations be used in modelling pressurization of adsorption beds, Gas Sep. Purif. 7 (3) (1993) 167–173.
[14] N. Sundaram, P.C. Wankat, Pressure drop effect in the pressurization and blowdown steps of Pressure Swing Adsorption, Chem. Eng. Sci. 43 (1) (1988) 123–129.
[15] G.M. Zhong, F. Meunier, S. Huberson, J.B. Chalfen, Pressurization of a single-component gas in an adsorption column, Chem. Eng. Sci. 47 (3) (1992) 543–550.
[16] L.R. Petzold, A Description of DASSL: A Differential/Algebraic System Solver, Sandia National Laboratories, Livermore, CA, 1982.
[17] M.H. Chahbani, Separation de gaz par Adsorption Modulée en Pression: modélisation des écoulements et de la cinétique de transfert de matière, thèse troisième cycle, INPL-ENSIC, France, 1996.
[18] J.M. Prausnitz, R.C. Reid, B.E. Poling, The Properties of Gases and Liquids, McGraw-Hill, New York, 1987.